
Disparate Vulnerability: on the Unfairness of Privacy Attacks Against Machine Learning

Mohammad Yaghini*, Bogdan Kulynych*, Carmela Troncoso
EPFL SPRING Lab

Abstract

A membership inference attack (MIA) against a machine learning model enables an attacker to determine whether a given data record was part of the model’s training dataset or not. Such attacks have been shown to be practical both in centralized and federated settings, and pose a threat in many privacy-sensitive domains such as medicine or law enforcement.

In the literature, the effectiveness of these attacks is invariably reported using metrics computed across the whole population. In this paper, we take a closer look at the attack’s performance *across different subgroups* present in the data distributions. We introduce a framework that enables us to efficiently analyze the vulnerability of machine learning models to MIA. We discover that even if the accuracy of MIA looks no better than random guessing over the whole population, subgroups are subject to *disparate vulnerability*, i.e., certain subgroups can be significantly more vulnerable than others. We provide a theoretical definition for MIA vulnerability which we validate empirically both on synthetic and real data.

1 Introduction

Machine learning models have been shown to be vulnerable to membership inference attacks (MIA). In these attacks, an adversary uses the outputs of a machine learning model to infer whether a given example was part of the training dataset. Such knowledge threatens individuals’ privacy when the classifier is associated to sensitive domains such as medical research [23], law enforcement [1], or financial services [15]. As MIA just relies on the model outputs, it is effective even when techniques to learn on encrypted inputs are in place, e.g., homomorphic encryption [3, 13, 16] or multi-party computation [5, 20, 24].

A series of works have shown the feasibility of MIA when the model is offered as a service [26], in federated settings [22]; moreover, the attacks can be effective even when the model is well generalized [19]. However, the attack effectiveness has so far only been evaluated by computing the accuracy of the attack *over the whole population*. In this paper we investigate whether such average-oriented evaluation actually reflects the impact of these attacks across *subgroups* of the population.

First, we introduce a new notion: *disparate vulnerability*, which, similarly to disparate impact [12] and disparate mistreatment [28] in fairness, captures the differential impact that privacy attacks have on subgroups. We propose a framework to quantify disparate vulnerability in an efficient manner, i.e., without requiring iterative training and testing of expensive models. This framework relies on a new definition, *MIA-indistinguishability*, that captures the resistance of a model to membership inference attacks. Based on this definition, we provide a method to compute the privacy loss for the population, or a given subgroup, in the presence of MIA adversaries. We show how these definitions relate to classical differential privacy [7, 10] and fairness [17, 28] notions.

* Authors contributed equally

Our theoretical analysis reveals that disparate vulnerability has two main roots. First, unbalanced training data across subgroups, i.e., disparate vulnerability will appear if a subgroup is under-sampled (or over-sampled). Second, disparate mistreatment [28] across subgroups; i.e., disparate vulnerability will appear if the model under attack yields dissimilar error rates for different subgroups.

We empirically evaluate these findings using synthetic datasets crafted to highlight the two causes above. We find that the difference in privacy loss between subgroups can be as large as 3.5 times in the most unfavorable conditions. We validate these findings on a classifier trained to predict the age of individuals in the ADULT dataset. We find that, regardless of the architecture of the classifier, underrepresented minorities such as Asian Pacific Americans or American Indian are more vulnerable to MIA than others, whereas the White majority is the least vulnerable to MIA: the difference is up to 12.5 times in the worst case. Finally, we show that a common technique to mitigate privacy leakage—differentially-private training [2, 14, 27] cannot effectively address disparate vulnerability.

2 Problem Setup

Let D be a *population*: the universe of labeled examples where each example represents an individual. We assume that this population contains disjoint *subgroups* $G_z \subset D$, for $z \in \{0, 1, \dots, m\}$. These represent different traits of the individuals, like races or genders.

We consider the binary classification setting, in which every example x has a label y in $\{0, 1\}$. We assume a binary *target classifier* $f(x)$ —the classifier under attack—that is trained on the *training dataset* X , sampled from D . On input $x, y \in D$, this classifier outputs a confidence for this example belonging to the positive class. Throughout this paper, unless explicitly said, the term classifier always refers to the target classifier.

A Membership Inference Attack (MIA) aims to determine whether some *target example* x^*, y^* was in the training dataset X , or not. We assume the adversary has *black-box* access to the classifier, i.e., they do not have *any* knowledge about the internals of the classifier, but they can request classification queries for an example and observe the output [26].

The MIA adversary’s goal can be thought of as reducing their uncertainty about a target example being in the training dataset, i.e., $x^*, y^* \in X$. For any given example from the population, x, y , we use a random variable $m \in \{0, 1\}$ to denote the adversary’s belief on whether the sample was in the training dataset ($m = 1$), or out ($m = 0$).

We also assume that the adversary does not have any prior knowledge on whether any x, y is included in the training dataset. More formally:

Assumption PK. For any $x \in X$: $\Pr[m = 1] = \Pr[m = 0]$

Additionally, we assume that the training dataset X contains no sampling class-bias. More formally:

Assumption CB. For any $y \in \{0, 1\}$: $\Pr[y = y \mid m = 1] = \Pr[y = y \mid m = 0]$

In this paper, we aim to characterize the *disparate vulnerability* of different subgroups to the MIA, i.e., the variation in the adversary’s probability to successfully attack examples from different subgroups.

2.1 MIA-indistinguishability

As a starting point for evaluating the attack success, we first characterize an ideal classifier that is *not* vulnerable to MIA.

A classifier is perfectly resistant to MIA attacks if, for every possible output of the classifier, from the adversary’s point of view any sample that could produce this output is as likely to be in the training set as out of the training set. Formally, we capture this through the notion of *perfect MIA-indistinguishability*, which we define both for the population and considering population subgroups.

Definition 1 (Perfect MIA-indistinguishability). The classifier $f(x)$ satisfies perfect MIA-indistinguishability if for any $p \in [0, 1]$ and $y \in \{0, 1\}$:

$$\Pr[m = 1 \mid f(\mathbf{x}) = p, y = y] = \Pr[m = 0 \mid f(\mathbf{x}) = p, y = y] \quad (1)$$

Statement 1 (Equivalent form). Given the assumptions CB and PK, the classifier $f(x)$ satisfies perfect MIA-indistinguishability iff for any $p \in [0, 1]$ and $y \in \{0, 1\}$:

$$\Pr[f(\mathbf{x}) = p \mid y = y, m = 1] = \Pr[f(\mathbf{x}) = p \mid y = y, m = 0] \quad (2)$$

Proof in Section S1.

Definition 2 (Perfect MIA-indistinguishability across subgroups). Let $z \in \{0, 1, \dots, m\}$ denote the membership of a sample \mathbf{x}, y in a given subgroup of the population. A classifier $f(\mathbf{x})$ satisfies perfect MIA-indistinguishability across the subgroups if for any $p \in [0, 1]$, $y \in \{0, 1\}$, and $z \in \{0, 1, \dots, m\}$:

$$\Pr[m = 1 \mid f(\mathbf{x}) = p, y = y, z = z] = \Pr[m = 0 \mid f(\mathbf{x}) = p, y = y, z = z] \quad (3)$$

Statement 2 (Equivalent form). Given the assumptions CB and PK, the classifier $f(\mathbf{x})$ satisfies perfect MIA-indistinguishability across subgroups iff for any $p \in [0, 1]$, $y \in \{0, 1\}$, and $z \in \{0, 1, \dots, m\}$:

$$\begin{aligned} & \Pr[f(\mathbf{x}) = p \mid y = y, z = z, m = 1] \Pr[z = z \mid y = y, m = 1] = \\ & \Pr[f(\mathbf{x}) = p \mid y = y, z = z, m = 0] \Pr[z = z \mid y = y, m = 0] \end{aligned} \quad (4)$$

Proof in Section S1.

We note that these are not the only possible ways to capture MIA resistance (see Section 4.1.1). However, as we show next, these notions enable us to easily establish connections with overfitting, sampling bias, and disparate mistreatment. They also provide a good basis to define efficient empirical measures of vulnerability.

3 Where Does the Vulnerability Come From?

In this section, we analyze the conditions needed to satisfy MIA-indistinguishability. We also compare the requirements to satisfy MIA-indistinguishability for the whole population and across subgroups.

First, take the classifier that satisfies perfect MIA-indistinguishability in the form of Equation 2. For $y = 1$, the classifier satisfies the following:

$$\underbrace{\Pr[f(\mathbf{x}) = p \mid y = 1, m = 1]}_{\text{TP (true-positive) over } X} = \underbrace{\Pr[f(\mathbf{x}) = p \mid y = 1, m = 0]}_{\text{TP over } \bar{X}}$$

Analogously, for $y = 0$. Hence, a MIA-resistant classifier has the same behavior with respect to both correct predictions and error rates on its training set and outside of it.

Contrast this to a classifier that is MIA-resistant across subgroups in the form of Equation 4. For $y = 1$:

$$\begin{aligned} & \underbrace{\Pr[f(\mathbf{x}) = p \mid y = 1, z = z, m = 1]}_{\text{TP on } X \cap G_z} \underbrace{\Pr[z = z \mid y = 1, m = 1]}_{\text{Positive-class } G_z \text{ proportion in } X} = \\ & \underbrace{\Pr[f(\mathbf{x}) = p \mid y = 1, z = z, m = 0]}_{\text{TP on } \bar{X} \cap G_z} \underbrace{\Pr[z = z \mid y = 1, m = 0]}_{\text{Positive-class } G_z \text{ proportion in } \bar{X}} \end{aligned}$$

Analogously, for $y = 0$. Let the proportions of G_z members in X and \bar{X} be the same. Then, the equality $\Pr[f(\mathbf{x}) = p \mid y = 1, z = z, m = 1] = \Pr[f(\mathbf{x}) = p \mid y = 1, z = z, m = 0]$ can be thought of a combination of *equalized odds* [17] and low *overfitting*—equal treatment of the subgroup across training and testing datasets.

However, in general the proportions are not equal, and a MIA-resistant classifier not only needs to not treat the subgroups equally, but also have the same rate of occurrence of the G_z members in the training set and outside. This means that if the training data has under-sampled (or over-sampled) one of the subgroups, the classifier is not MIA-resistant. Interestingly, it is possible for a G_z with an imbalanced TP probability to compensate with over-representation, i.e. a higher positive-class G_z proportion in X , thus maintaining MIA-resistance.

4 Measures of Disparate Vulnerability

Based on the theoretical notions in Section 2, we propose two means to evaluate in practice the vulnerability of a given classifier to MIA: *privacy loss*, which measures how far is a classifier to meet the ideal conditions, and *efficient attack simulations*, which empirically measure the vulnerability by simulating attacks.

4.1 Privacy Loss

In practice, it is unlikely that a classifier can satisfy the conditions from Section 3. Thus, by how much the classifier deviates from these conditions can be a measure of its vulnerability to MIA. Inspired by differential privacy and individual fairness [11], we measure this deviation using the ℓ_∞ -relative metric, between the sides of Equation 2 and 4. To capture the worst-case vulnerability, we take the maximum divergence across classes $y \in \{0, 1\}$:

Definition 3 (Average MIA-privacy loss).

$$\bar{L}^{\text{MIA}} = \sup_{y \in \{0,1\}} \left| \log \frac{\mathbb{E}[f(\mathbf{x}) \mid y = y, \mathbf{m} = 1]}{\mathbb{E}[f(\mathbf{x}) \mid y = y, \mathbf{m} = 0]} \right| \quad (5)$$

Definition 4 (Average MIA-privacy loss of a subgroup). For a given $z \in \{0, 1, \dots, m\}$:

$$\bar{L}_z^{\text{MIA}} = \sup_{y \in \{0,1\}} \left| \log \frac{\mathbb{E}[f(\mathbf{x}) \mid y = y, z = z, \mathbf{m} = 1] \Pr[z = z \mid y = y, \mathbf{m} = 1]}{\mathbb{E}[f(\mathbf{x}) \mid y = y, z = z, \mathbf{m} = 0] \Pr[z = z \mid y = y, \mathbf{m} = 0]} \right| \quad (6)$$

The closer the privacy loss is to zero, the more similar are the results of the classifier on training examples to those on examples out of training. Thus, in both cases, small privacy loss (close to zero) indicates strong resistance to MIA.

We show in Algorithm 1 how these losses can be compute empirically. Let X be the training set of the classifier $f(\mathbf{x})$, and X_{test} be a test set, not used for training, nor hyper-parameter selection. Assume that both X and X_{test} have the same proportion of y -samples for $y \in \{0, 1\}$. First, we create samples from X and X_{test} . Second, for each true class we 1) compute the ratio of subgroup samples in X and X_{test} (r_{in} and r_{out} , respectively); 2) compute the average of the classifier's outputs in X and X_{test} (\bar{p}_{in} and \bar{p}_{out} , respectively); and 3) compute the privacy loss. (Note that to obtain the general MIA-privacy loss it suffices to consider $G_z = X$)

Algorithm 1 Empirical computation of Equation 6

Require: $n \leq \min\{|X|, |X_{\text{test}}|\}$

procedure COMPUTEAVGLOSS($f, X, X_{\text{test}}, G_z; n$)

 Sample $X_{in} \stackrel{\$}{\leftarrow} X, X_{out} \stackrel{\$}{\leftarrow} X_{\text{test}}$ s.t. $|X_{in}| = |X_{out}| = n$

$c_t := \{\}$

for $t \in \{0, 1\}$ **do**

$$r_{in} := \frac{|\{\mathbf{x}, y \in G_z \cap X_{in} \mid y = t\}|}{|\{\mathbf{x}, y \in X_{in} \mid y = t\}|}$$

$$r_{out} := \frac{|\{\mathbf{x}, y \in G_z \cap X_{out} \mid y = t\}|}{|\{\mathbf{x}, y \in X_{out} \mid y = t\}|}$$

$$\bar{p}_{in} := \sum_{\mathbf{x}, y \in \{\mathbf{x}, y \in G_z \cap X_{in} \mid y = t\}} \frac{f(\mathbf{x})}{|\{\mathbf{x}, y \in G_z \cap X_{in} \mid y = t\}|}$$

$$\bar{p}_{out} := \sum_{\mathbf{x}, y \in \{\mathbf{x}, y \in G_z \cap X_{out} \mid y = t\}} \frac{f(\mathbf{x})}{|\{\mathbf{x}, y \in G_z \cap X_{out} \mid y = t\}|}$$

$$c_t := \left| \log \frac{\bar{p}_{in} \cdot r_{in}}{\bar{p}_{out} \cdot r_{out}} \right|$$

return $\max\{c_0, c_1\}$

4.1.1 Discussion

We discuss the rationale behind the choice of these measures.

Expectation vs. Probability. A natural way to express the deviation from the perfect MIA-indistinguishability (Equation 2 and 4) would be to use the probability of $f(\mathbf{x}) = p$ rather than the expected value of $f(\mathbf{x})$. For example, extending Equation 2, we obtain:

Definition 5 (Worst-case MIA privacy loss).

$$L^{\text{MIA}} = \sup_{\substack{p \in [0,1] \\ y \in \{0,1\}}} \left| \log \frac{\Pr[f(\mathbf{x}) = p \mid y = y, m = 1]}{\Pr[f(\mathbf{x}) = p \mid y = y, m = 0]} \right| \quad (7)$$

As $p \in [0, 1]$ is continuous, computing this expression in practice is prone to numerical instability. Indeed, a straightforward way to compute this value is to discretize $[0, 1]$ into a fixed number of bins b . However, in our experiments, we observe significant difference in distributions of loss values when varying the number of bins.

Taking the expectation makes the computation feasible and stable (see above). However, it does not capture the worst-case scenario. Assume that the ratio of expectations of $f(\mathbf{x})$ over all values of $p \in [0, 1]$ is close to one (i.e., the classifier is resistant to MIA in the average-loss notion). There could be a particular value of p for which the ratio of probabilities given $m = 1$ and $m = 0$ is significantly higher or lower than one. Hypothetically, the adversary could use this value to distinguish whether some example was in or out of the training set. Yet, as demonstrated by our experiments, the expectation-based notion still provides a useful lower bound on the vulnerability.

Differential-Privacy Loss Training a classifier $f(x)$ using a *differentially-private (DP)* algorithm [7, 10] naturally results in bounds on general vulnerability of the classifier to MIA. We compare this privacy notion to our privacy measures.

The classical differential privacy definition refers to databases:

Definition 6 (Differential privacy [7, 9, 10]). A probabilistic function $g(X) \in Y$ satisfies ε -differential privacy if for any two *neighbouring databases* X and X' , differing by one element, the DP loss is bounded by ε :

$$L_{X,X'}^{\text{DP}} \leq \varepsilon$$

From this definition, Dwork and Roth derive a commonly-used privacy-loss notion [8]. We provide an alternative definition to draw clearer parallels with MIA-privacy loss:

Definition 7 (Differential-privacy loss). For a probabilistic function $g(X) \in Y$ that takes as input a *database* $X \subset 2^D$, we define the DP loss of two databases X and X' as follows:

$$L_{X,X'}^{\text{DP}} = \sup_{S \subset Y} \left| \log \frac{\Pr[g(X) \in S]}{\Pr[g(X') \in S]} \right| \quad (8)$$

Even though our privacy-loss notions are similar to the DP loss in form and spirit, they are not trivially connected.

Let us denote by g the probabilistic training procedure that takes as input a dataset X and outputs a classifier f . Assume that g satisfies ε -differential privacy with a small ε (note that by the DP post-processing property [8], the classifier $f(\mathbf{x})$ also satisfies ε -differential privacy). Intuitively, this means that outputs of the training procedure g do not differ by much if any given record \mathbf{x}, y was included in the training dataset X or not. As the training procedure is probabilistic, computing the corresponding DP loss would require sampling neighbouring databases X and X' , and training respective classifiers f and f' . Hence, this loss is not suitable for evaluating after the fact of training.

Assume that the classifier has the MIA-privacy loss bounded by a small ε : $\bar{L}^{\text{MIA}} < \varepsilon$. Intuitively, this too means that the classifier’s outputs do not differ by much if a given record \mathbf{x}, y was included in the training dataset X , or not. Computing this loss empirically, unlike the DP loss, requires creating two samples from the actual training dataset X and a test dataset X_{test} , and computing the average of the classifier’s outputs. This procedure is efficient, and does not involve retraining multiple classifiers.

4.2 Efficient Attack Simulation

Another way to evaluate a classifier’s vulnerability to MIA is empirically measure the attack’s success. The pioneering black-box attack proposed by Shokri et al. [26] relies on computing multiple *shadow models* that have the same architecture as the target model. This can become extremely expensive, especially for deep neural networks. In our security-evaluation scenario, however, where the goal is to obtain worst-case security guarantees, some of these assumptions can be relaxed.

In this evaluation, following the method in Nasr et al. [21], we allow the adversary to have some background knowledge on X . They have access to a *compromised* subsample of the training dataset X^c and a compromised subsample of the test dataset X_{test}^c . They also have the output of the target classifier $f(x)$ for each example in the compromised datasets. The adversary uses these datasets to train a machine-learning classifier that distinguishes whether an example x, y was in or out of the training dataset by only looking at its true class y and the prediction $p = f(x)$. Such an attack, unlike the one by Shokri et al. [26], requires training only one classifier. We provide the detailed algorithm for simulating this attacker in Algorithm 3 (Section S4).

In our experiments, we use the accuracy of the attacker on the *non-compromised part* of X and X_{test} to measure MIA vulnerability. For more reliable estimates, several attacker classifiers can be trained on different compromised subsamples.

5 Empirical Evaluation

Our experiments aim to answer the following questions. First, are our hypothesis behind the origin of disparate vulnerability correct? Second, is MIA’s success proportional to the values of MIA-privacy loss? Third, is there disparate vulnerability towards MIA? If yes, for which models? Fourth, when and by how much the existing privacy-enhancing strategies help in reducing disparate vulnerability?

5.1 Experimental Setup

Evaluated Model Architectures We consider the following model architectures, which represent typical classes of models in machine learning: ℓ_2 -regularized Logistic Regression (LR), SVM with the RBF-kernel (SVM), and a single-hidden-layer feed-forward Neural Network (NN) with different configurations. We use scikit-learn for their implementations [25].

We also consider two models trained with differential privacy. First, we employ the state-of-the-art Approximate Minima Perturbation method [14], and Private Perturbation-based Convex SGD [27] to train private LR model (LR-AMP-DP and LR-PSGD-DP, respectively), both with $\epsilon = 1$. We use the open-source implementation² of both algorithms by Iyengar et al. [14]

Computation of Vulnerability Measures For each model, we compute the privacy loss on subsamples from X and X_{test} using the COMPUTEAVGLOSS procedure (Algorithm 1). We run both COMPUTEAVGLOSS and MIA attack simulations on 30 different subsamples of the datasets. We consider that to distinguish samples in and out of the training dataset, the adversary uses an XGBoost tree-boosting classifier [4] (see Section S5.1) for details). We set the size of the subsamples both for privacy loss and attack simulations to 20% of $|X|$.

In our results, we represent disparate vulnerability by reporting the *largest difference in average MIA-privacy loss (resp., attacker accuracy)* across all subgroups, as this represents the worst-case scenario.

In Section 4 we present the vulnerability measures in the binary-class classification setting. Yet, the target classifier we use in this evaluation is multi-class. We note that generalizing to multi-class is straightforward. We refer the reader to Section S3 for details.

5.2 Evaluation on Synthetic Datasets

Dataset To empirically evaluate our hypotheses in Section 3, we evaluate the disparate vulnerability of several models on two synthetic datasets X_D and X_{ND} . Both datasets have 50K samples, divided equally into 5 subgroups with 10 features and 10 class labels. The features are sampled from the same normal distribution $\mathcal{N}(\mathbf{0}, 2\mathbf{I})$.

We aim to evaluate the effects of overfitting (unequal error behaviour between X and \bar{X}) and subgroup-sampling disparity (Section 3). We thus consider two non-overfitting models: LR, a neural network with 6 neurons in the hidden layer, and a deliberately overfitting NN with 500 neurons (NN-500). We include performance details of the models in Table S2 for reference. To control for sampling disparity, X_{ND} is split 60/40% for train and test across all subgroups. Subgroup $X_D \cap G_2$ has a 70/30% split and the rest of the subgroups are split 60/40%.

²<https://github.com/sunblaze-ucb/dpml-benchmark>

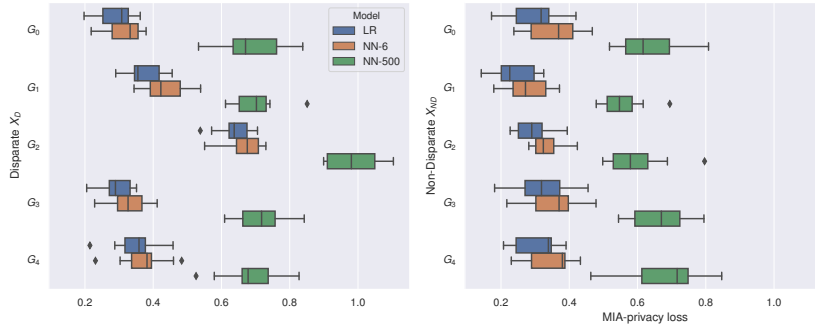


Figure 1: Adverse effects of overfitting and under-/over-sampling on MIA-privacy (subgroup G_2 is under-sampled in the training dataset), and the disparity of these effects on different sub-populations

Figure 1 shows our results. We observe that, indeed, the subgroup with a different ratio in test/train (G_2) suffers a higher privacy loss for all models. Overfitting increases the privacy loss for all subgroups, but the impact is still disparate with G_2 taking the biggest hit.

5.3 Evaluation on Real Data

Dataset For our realistic evaluation use the well-known ADULT dataset [18] from the UCI Machine Learning Repository [6]. This dataset contains attributes about individuals that could be considered sensitive and/or susceptible to discrimination: *education*, *marital status*, *occupation*, etc. As MIA are known to be ineffective against binary classifiers [26], we modify the dataset to create a non-binary target by bucketizing the *age* feature into 10 quantile-based buckets. We train the considered models to predict the exact age bucket given all the other features. We call this dataset *ADULT-10*.

We take as subgroups G_z the race groups³ present in the dataset: “*White*” (41,762 examples), “*Black*” (4,685), “*Asian or Pacific Islander*” (1,519), “*American Indian / Eskimo*” (470), and “*Other*” (406).

In this evaluation, as is common in reality, we do not control for subgroup-sampling bias. Thus, we split the full dataset into train and test sets at random (70/20%, 34,189 and 14,652 examples, respectively).

Models Empirically, we find that the baseline accuracy (predicting the most-frequent class) for this task is 12%. All the models we consider achieve at least 24–27% accuracy on the test set. For the NN architectures, we train the base model with 6 hidden neurons in the hidden layer, and additionally, we train three deliberately overfitting models with 50, 100, and 500 neurons. All other models do not exhibit signs of significant overfitting. Table 1 contains the summaries of models’ performance; we refer to Section S5.1 for the hyper-parameter values and strategies for their selection.

Results We show the average measurements over multiple runs in Table 1. First, we find that higher privacy loss values, and disparate vulnerability in terms of loss (loss disparity), correspond to both higher attack accuracy and disparate vulnerability in terms of the attack’s success (attack disparity). In particular, as the cases of NN-50, NN-100, NN-500 show, overfitting dramatically increases the privacy loss and the attack accuracy, both in terms of averages and their disparities. Second, we find that for all considered models, the privacy losses are significantly higher for subgroups with smaller representation. We show the breakdown of the MIA-privacy losses by subgroups for several of the classifiers in Figure 2, and refer to Section S5.3 for detailed results for all classifiers. In terms of attack accuracy, we find that, even if the average attack accuracy is 50%, the attack can impact different groups with the difference of as much as 6–12 percentage points; especially so when a model is overfitting. Third, as Figure 2 shows, the state-of-the-art algorithms for private training do not mitigate the disparate vulnerability.

³Values of the *race* attribute are taken from the dataset

Table 1: Results on ADULT-10 dataset. Columns: *Test acc.*—accuracy of the target model on the test dataset, *Train acc.*—accuracy of the target model on the train dataset; *Loss*—MIA-privacy loss \bar{L}^{MIA} , average over 30 replications; *Loss disp.*—max. absolute difference (*disparity*) in MIA-privacy loss \bar{L}_z^{MIA} between any two subgroups z, z' ; *Attack acc.*—accuracy of a simulated attacker, average over 30 attacks; *Attack disp.*—max. absolute difference in attack accuracy between any two subgroups.

| Model | Test acc. | Train acc. | Loss | Loss disp. | Attack acc. | Attack disp. |
|------------|-----------|------------|------|------------|-------------|--------------|
| LR | 0.28 | 0.29 | 1.50 | 2.69 | 0.50 | 0.07 |
| SVM | 0.26 | 0.26 | 1.76 | 3.00 | 0.50 | 0.06 |
| NN-6 | 0.29 | 0.30 | 2.27 | 3.96 | 0.50 | 0.07 |
| LR-AMP-DP | 0.24 | 0.25 | 1.99 | 3.79 | 0.50 | 0.08 |
| LR-PSGD-DP | 0.20 | 0.20 | 1.71 | 3.13 | 0.50 | 0.07 |
| NN-50 | 0.28 | 0.34 | 2.70 | 4.87 | 0.51 | 0.06 |
| NN-100 | 0.27 | 0.38 | 3.06 | 5.89 | 0.53 | 0.07 |
| NN-500 | 0.26 | 0.43 | 3.83 | 7.64 | 0.56 | 0.12 |

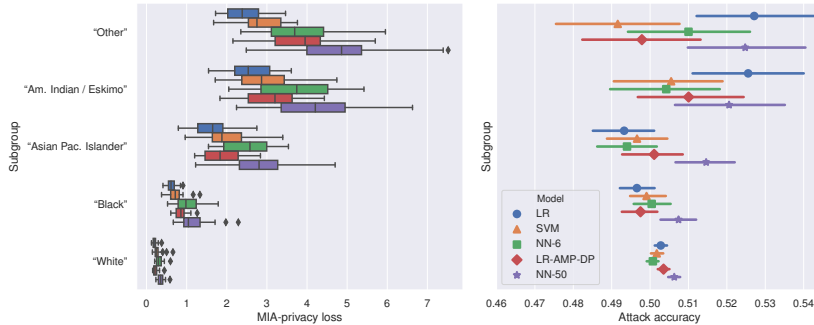


Figure 2: MIA-privacy losses and accuracy of simulated attacks across subgroups on ADULT-10. Attack-accuracy error bars represent 95% bootstrap CI over the full set of measurements.

6 Conclusions

We have shown that discrimination caused by machine learning models is not limited to the impact of predictions on different subgroups. Differences in the number of samples used in training for different subgroups, or in the errors that the classifier makes for these subgroups, can also cause *disparate vulnerability* to privacy attacks on machine learning models.

We have further shown that this new source of unfairness is closely related to the disparate mistreatment. As such, it is unlikely that one can have calibrated classifiers that ensure equal privacy for all participants in a dataset. Moreover, we have also shown that the nature of this new form of discrimination, in the boundary between fairness and privacy, cannot be tackled with existing privacy-protection techniques. It therefore opens a new research question: is it possible to obtain both fundamental rights, privacy and non-discrimination, simultaneously? Our study has focused on a concrete attack, membership inference. However, similarly to the different flavours of fairness, there exist other attacks such as model inversion or attribute inference, whose analysis requires different privacy notions than MIA. Are any of these notions compatible with fairness? We hope that our work serves as catalyzer for future research that addresses these questions.

References

- [1] Predpol – predictive policing. <https://www.predpol.com/>. Accessed: March 22, 2022.
- [2] M. Abadi, A. Chu, I. J. Goodfellow, H. B. McMahan, I. Mironov, K. Talwar, and L. Zhang. Deep learning with differential privacy. In *Proceedings of the 2016 ACM SIGSAC Conference on Computer and Communications Security, Vienna, Austria, October 24-28, 2016*, 2016.
- [3] H. Chen, R. Gilad-Bachrach, K. Han, Z. Huang, A. Jalali, K. Laine, and K. E. Lauter. Logistic regression over encrypted data from fully homomorphic encryption. *IACR Cryptology ePrint Archive*, 2018.
- [4] T. Chen and C. Guestrin. XGBoost: A scalable tree boosting system. In *Proceedings of the 22nd ACM SIGKDD International Conference on Knowledge Discovery and Data Mining, San Francisco, CA, USA, August 13-17, 2016*, 2016.
- [5] V. Chen, V. Pastro, and M. Raykova. Secure computation for machine learning with SPDZ. *CoRR*, abs/1901.00329, 2019.
- [6] D. Dheeru and E. Karra Taniskidou. UCI machine learning repository, 2017. URL <http://archive.ics.uci.edu/ml>.
- [7] C. Dwork. Differential privacy. In *Encyclopedia of Cryptography and Security, 2nd Ed.* 2011.
- [8] C. Dwork and A. Roth. The algorithmic foundations of differential privacy. *Foundations and Trends in Theoretical Computer Science*, 2014.
- [9] C. Dwork and G. N. Rothblum. Concentrated differential privacy. *CoRR*, abs/1603.01887, 2016. URL <http://arxiv.org/abs/1603.01887>.
- [10] C. Dwork, F. McSherry, K. Nissim, and A. D. Smith. Calibrating noise to sensitivity in private data analysis. In *Theory of Cryptography, Third Theory of Cryptography Conference, TCC, 2006*.
- [11] C. Dwork, M. Hardt, T. Pitassi, O. Reingold, and R. S. Zemel. Fairness through awareness. In *Innovations in Theoretical Computer Science*, 2012.
- [12] M. Feldman, S. A. Friedler, J. Moeller, C. Scheidegger, and S. Venkatasubramanian. Certifying and removing disparate impact. In *Proceedings of the 21th ACM SIGKDD International Conference on Knowledge Discovery and Data Mining*, 2015.
- [13] T. Graepel, K. E. Lauter, and M. Naehrig. ML confidential: Machine learning on encrypted data. In *Information Security and Cryptology - ICISC*, pages 1–21, 2012.
- [14] R. Iyengar, J. P. Near, D. Song, O. Thakkar, A. Thakurta, and L. Wang. Towards practical differentially private convex optimization. In *Towards Practical Differentially Private Convex Optimization*, page 0. IEEE, 2019.
- [15] A. E. Khandani, A. J. Kim, and A. W. Lo. Consumer credit-risk models via machine-learning algorithms. *Journal of Banking & Finance*, 2010.
- [16] M. Kim, Y. Song, S. Wang, Y. Xia, and X. Jiang. Secure logistic regression based on homomorphic encryption: Design and evaluation. *JMIR medical informatics*, 6(2):e19, 2018.
- [17] J. M. Kleinberg, S. Mullainathan, and M. Raghavan. Inherent trade-offs in the fair determination of risk scores. In *ITCS*, 2017.
- [18] R. Kohavi. Scaling up the accuracy of naive-bayes classifiers: A decision-tree hybrid. In *Proceedings of the Second International Conference on Knowledge Discovery and Data Mining (KDD-96), Portland, Oregon, USA, 1996*.
- [19] Y. Long, V. Bindschaedler, L. Wang, D. Bu, X. Wang, H. Tang, C. A. Gunter, and K. Chen. Understanding membership inferences on well-generalized learning models. *arXiv preprint arXiv:1802.04889*, 2018.
- [20] P. Mohassel and Y. Zhang. SecureML: A system for scalable privacy-preserving machine learning. In *IEEE Symposium on Security and Privacy, SP*, 2017.
- [21] M. Nasr, R. Shokri, and A. Houmansadr. Machine learning with membership privacy using adversarial regularization. In *ACM SIGSAC Conference on Computer and Communications Security, CCS*, pages 634–646, 2018.

- [22] M. Nasr, R. Shokri, and A. Houmansadr. Comprehensive privacy analysis of deep learning: Stand-alone and federated learning under passive and active white-box inference attacks. In *IEEE Symposium on Security and Privacy, SP*, 2018.
- [23] Z. Obermeyer and E. J. Emanuel. Predicting the future—big data, machine learning, and clinical medicine. *The New England journal of medicine*, 2016.
- [24] O. Ohrimenko, F. Schuster, C. Fournet, A. Mehta, S. Nowozin, K. Vaswani, and M. Costa. Oblivious multi-party machine learning on trusted processors. In *USENIX Security Symposium*, 2016.
- [25] F. Pedregosa, G. Varoquaux, A. Gramfort, V. Michel, B. Thirion, O. Grisel, M. Blondel, P. Prettenhofer, R. Weiss, V. Dubourg, J. Vanderplas, A. Passos, D. Cournapeau, M. Brucher, M. Perrot, and E. Duchesnay. Scikit-learn: Machine Learning in Python . *Journal of Machine Learning Research*, 2011.
- [26] R. Shokri, M. Stronati, C. Song, and V. Shmatikov. Membership inference attacks against machine learning models. In *IEEE Symposium on Security and Privacy, SP*, 2017.
- [27] X. Wu, F. Li, A. Kumar, K. Chaudhuri, S. Jha, and J. F. Naughton. Bolt-on differential privacy for scalable stochastic gradient descent-based analytics. In *Proceedings of the 2017 ACM International Conference on Management of Data, SIGMOD Conference 2017, Chicago, IL, USA, May 14-19, 2017*, 2017.
- [28] M. B. Zafar, I. Valera, M. Gomez-Rodriguez, and K. P. Gummadi. Fairness beyond disparate treatment & disparate impact: Learning classification without disparate mistreatment. In *WWW*, 2017.

Supplementary Information: Disparate Vulnerability: on the Unfairness of Privacy Attacks Against Machine Learning

Mohammad Yaghini*, Bogdan Kulynych*, Carmela Troncoso
EPFL SPRING Lab

S1 Proofs of Equivalent Forms of the MIA-Indistinguishability Notions

Lemma 1. Given the assumptions CB and PK, the following holds:

$$\Pr[m = 1 \mid y = y] = \Pr[m = 0 \mid y = y] \quad (\text{S1})$$

Proof. By Bayes theorem. □

S1.1 Proof of Statement 1

Proof. From Equation 1, by Bayes theorem we get:

$$\begin{aligned} \Pr[f(\mathbf{x}) = p \mid y = y, m = 1] \Pr[m = 1 \mid y = y] = \\ \Pr[f(\mathbf{x}) = p \mid y = y, m = 0] \Pr[m = 0 \mid y = y] \end{aligned}$$

By Lemma 1, we get Equation 2. □

S1.2 Proof of Statement 2

Proof. This proof is analogous to that of Equation 2. From Equation 3, by Bayes theorem we get:

$$\begin{aligned} \Pr[f(\mathbf{x}) = p \mid y = y, z = z, m = 1] \Pr[m = 1 \mid y = y, z = z] = \\ \Pr[f(\mathbf{x}) = p \mid y = y, z = z, m = 0] \Pr[m = 0 \mid y = y, z = z] \\ \Pr[f(\mathbf{x}) = p \mid y = y, z = z, m = 1] \Pr[z = z \mid y = y, m = 1] \Pr[m = 1 \mid y = y] = \\ \Pr[f(\mathbf{x}) = p \mid y = y, z = z, m = 0] \Pr[z = z \mid y = y, m = 0] \Pr[m = 0 \mid y = y] \end{aligned}$$

By Lemma 1, we get Equation 4. □

S2 Decomposition of MIA-Indistinguishability Conditions

In this section, we provide a more verbose way to interpret the MIA-indistinguishability conditions.

Statement 3 (Decomposition). Either the left or the right hand side of Equation 4 can be decomposed in the following way:

$$\begin{aligned} \Pr[f(\mathbf{x}) = p \mid y = y, z = z, m = m] \Pr[z = z \mid y = y, m = m] = \\ \frac{\Pr[f(\mathbf{x}) = p \mid z = z, m = m]}{\Pr[f(\mathbf{x}) = p \mid z = z]} \frac{\Pr[y = y \mid z = z]}{\Pr[y = y]} \Pr[z = z \mid m = m] \Pr[f(\mathbf{x}) = p \mid y = y, z = z] \end{aligned} \quad (\text{S2})$$

*Authors contributed equally

Proof. Using Bayes Theorem and the law of total probabilities, and using assumption CB (which implies $y \perp m$) the first term can be simplified as:

$$\Pr[f(\mathbf{x}) = p \mid y = y, z = z, m = m] = \frac{\Pr[f(\mathbf{x}) = p \mid z = z, m = m] \Pr[y = y \mid z = z]}{\Pr[y = y \mid z = z, m = m] \Pr[f(\mathbf{x}) = p \mid z = z]} \Pr[f(\mathbf{x}) = p \mid y = y, z = z]$$

and the second term can be decomposed in a similar manner into the following:

$$\Pr[z = z \mid y = y, m = m] = \frac{\Pr[m = m \mid z = z] \Pr[y = y \mid z = z, m = m] \Pr[z = z]}{\Pr[y = y] \Pr[m = m]}$$

Multiplying the two terms cancels the $\Pr[y = y \mid z = z, m = m]$ term. We further simplify the result with Bayes and total probability rules to arrive at the desired decomposition. \square

Note the various terms in equation S2:

$$\underbrace{\frac{\Pr[f(\mathbf{x}) = p \mid z = z, m = m]}{\Pr[f(\mathbf{x}) = p \mid z = z]}}_{r_{\text{overfitting}}} \underbrace{\frac{\Pr[y = y \mid z = z]}{\Pr[y = y]}}_{r_{\text{data bias}}} \underbrace{\Pr[z = z \mid m = m]}_{r_{\text{sampling bias}}} \Pr[f(\mathbf{x}) = p \mid y = y, z = z]. \quad (\text{S3})$$

S3 Generalizations to the Multi-Class Setting

The theoretical notions we use can be generalized to the multi-class classification setting in a straightforward way. Let $Y = \{0, 1, \dots, k\}$ be the set of possible output classes, and $f_t(\mathbf{x})$ denote the confidence that a classifier assigns to \mathbf{x} as belonging to class $t \in Y$.

First, we extend the sampling class-bias assumption:

Assumption MCB. For any $t \in Y$: $\Pr[y = t \mid m = 1] = \Pr[y = t \mid m = 0]$

Second, we provide multi-class generalizations for the MIA-indistinguishability notions and their equivalent forms.

Definition 8 (Perfect MIA-indistinguishability). The classifier $f(\mathbf{x})$ satisfies perfect MIA-indistinguishability iff for any $p \in [0, 1]$ and $t, t' \in Y$:

$$\Pr[m = 1 \mid f_t(\mathbf{x}) = p, y = t'] = \Pr[m = 0 \mid f_t(\mathbf{x}) = p, y = t'] \quad (\text{S4})$$

Statement 4 (Equivalent form). Given the assumptions MCB and PK, the classifier $f(\mathbf{x})$ satisfies perfect MIA-indistinguishability iff for any $p \in [0, 1]$ and $t, t' \in Y$:

$$\Pr[f_t(\mathbf{x}) = p \mid y = t', m = 1] = \Pr[f_t(\mathbf{x}) = p \mid y = t', m = 0] \quad (\text{S5})$$

Proof. Analogous to the proof of Statement 1 in Section S1. \square

Definition 9 (Perfect MIA-indistinguishability across subgroups). Let $z \in \{0, 1, \dots, m\}$ denote the membership of a sample \mathbf{x}, y in a given subgroup of the population. A classifier $f(\mathbf{x})$ satisfies perfect MIA-indistinguishability across the subgroups iff for any $p \in [0, 1]$, $t, t' \in Y$, and $z \in \{0, 1, \dots, m\}$:

$$\Pr[m = 1 \mid f_t(\mathbf{x}) = p, y = t', z = z] = \Pr[m = 0 \mid f_t(\mathbf{x}) = p, y = t', z = z] \quad (\text{S6})$$

Statement 5 (Equivalent form). Given the assumptions MCB and PK, the classifier $f(\mathbf{x})$ satisfies perfect MIA-indistinguishability across subgroups iff for any $p \in [0, 1]$, $t, t' \in Y$, and $z \in \{0, 1, \dots, m\}$:

$$\begin{aligned} & \Pr[f_t(\mathbf{x}) = p \mid y = t', z = z, m = 1] \Pr[z = z \mid y = t', m = 1] = \\ & \Pr[f_t(\mathbf{x}) = p \mid y = t', z = z, m = 0] \Pr[z = z \mid y = t', m = 0] \end{aligned} \quad (\text{S7})$$

Proof. Analogous to the proof of Statement 2 in Section S1. \square

Finally, we provide the generalized version of MIA-privacy losses.

Algorithm 2 Empirical computation of Equation S9 (multi-class setting)

Require: $n \leq \min\{|X|, |X_{\text{test}}|\}$ **procedure** COMPUTEAVGLOSS($X, X_{\text{test}}, z; n$)Sample $X_{in} \stackrel{\$}{\leftarrow} X, X_{out} \stackrel{\$}{\leftarrow} X_{\text{test}}$ s.t. $|X_{in}| = |X_{out}| = n$ $c_{t,t'} := \{\}$ **for** $t, t' \in Y \times Y$ **do**

$$r_{in} := \frac{|\{\mathbf{x}, y \in G_z \cap X_{in} \mid y = t\}|}{|\{\mathbf{x}, y \in X_{in} \mid y = t\}|}$$

$$r_{out} := \frac{|\{\mathbf{x}, y \in G_z \cap X_{out} \mid y = t\}|}{|\{\mathbf{x}, y \in X_{out} \mid y = t\}|}$$

$$\bar{p}_{in} := \sum_{\mathbf{x}, y \in \{\mathbf{x}, y \in G_z \cap X_{in} \mid y=t\}} \frac{f_{t'}(\mathbf{x})}{|\{\mathbf{x}, y \in X_{in} \cap G_z \mid y = t\}|}$$

$$\bar{p}_{out} := \sum_{\mathbf{x}, y \in \{\mathbf{x}, y \in G_z \cap X_{out} \mid y=t\}} \frac{f_{t'}(\mathbf{x})}{|\{\mathbf{x}, y \in X_{out} \cap G_z \mid y = t\}|}$$

$$c_{t,t'} := \left| \log \frac{\bar{p}_{in} \cdot r_{in}}{\bar{p}_{out} \cdot r_{out}} \right|$$

return $\max_{t,t'} \{c_{t,t'}\}$

Definition 10 (Average MIA privacy loss).

$$\bar{L}^{\text{MIA}} = \sup_{t,t' \in Y} \left| \log \frac{\mathbb{E}[f_t(\mathbf{x}) \mid y = t', \mathbf{m} = 1]}{\mathbb{E}[f_t(\mathbf{x}) \mid y = t', \mathbf{m} = 0]} \right| \quad (\text{S8})$$

Definition 11 (Average MIA privacy loss of a subgroup).

$$\bar{L}_z^{\text{MIA}} = \sup_{t,t' \in Y} \left| \log \frac{\mathbb{E}[f_t(\mathbf{x}) \mid y = t', z = z, \mathbf{m} = 1] \Pr[z = z \mid y = t', \mathbf{m} = 1]}{\mathbb{E}[f_t(\mathbf{x}) \mid y = t', z = z, \mathbf{m} = 0] \Pr[z = z \mid y = t', \mathbf{m} = 0]} \right| \quad (\text{S9})$$

Algorithm 2 details the procedure of computing the MIA-privacy loss in the multi-class setting.

S4 Attacker-Simulation Algorithm

Algorithm 3 details the algorithm for simulating a MIA attacker in the binary-class setting, and Algorithm 4—in the multi-class setting. First, we sample compromised parts of X and X_{test} , designated as adversary’s background knowledge. Second, we obtain the outputs of the target classifier $f(\mathbf{x})$ on the compromised samples, and arrange these outputs and true class values of the compromised examples into a form of a machine-learning training dataset, along with membership labels: A label of a sample that was in training is 1, and that of a sample that was out is 0. In the multi-class setting, we also encode the true class of each compromised example as a one-hot vector (denoted as $\text{onehot}(y)$). Third, we train a machine-learning classifier on this data to learn to distinguish samples that were in the training set from those out of the training set.

S5 Evaluation Details

S5.1 Model Hyper-Parameters

Table S1 lists the hyper-parameters used for the target and the attacker’s models. We select the hyper-parameters of LR, SVM, and NN-6 using 5-fold cross-validation on the training part of the ADULT-10 dataset. In the case of LR and SVM, we consider several values of the regularization parameter C (0.01, 0.1, 1); in the case of NN-6, the regularization parameter α (0.01, 0.1, 1) and the dimensionality of the hidden layer (4, 5, 6, 10, 12, 20).

Algorithm 3 Attacker-simulation procedure (binary-class setting)

Require: $n \leq \min\{|X|, |X_{\text{test}}|\}$

Require: train: an ML training procedure

procedure SIMATTACKER($f, X, X_{\text{test}}; n$)

Sample $X^c \stackrel{\$}{\leftarrow} X, X_{\text{test}}^c \stackrel{\$}{\leftarrow} X_{\text{test}}$ s.t. $|X^c| = |X_{\text{test}}^c| = n$

$$X_{in}^a = \begin{bmatrix} f(x_0) | y_0 \\ f(x_1) | y_1 \\ \vdots \\ f(x_n) | y_n \end{bmatrix}, \begin{bmatrix} 1 \\ 1 \\ \vdots \\ 1 \end{bmatrix}$$

$$X_{out}^a = \begin{bmatrix} f(x'_0) | y'_0 \\ f(x'_1) | y'_1 \\ \vdots \\ f(x'_n) | y'_n \end{bmatrix}, \begin{bmatrix} 0 \\ 0 \\ \vdots \\ 0 \end{bmatrix}$$

for all $x_i, y_i \in X^c$ and $x'_i, y'_i \in X_{\text{test}}^c$.

$a \leftarrow \text{train} \left(\begin{bmatrix} X_{in}^a \\ X_{out}^a \end{bmatrix} \right)$

return a

Algorithm 4 Attacker-simulation procedure (multi-class setting)

Require: $n \leq \min\{|X|, |X_{\text{test}}|\}$

Require: train: an ML training procedure

procedure SIMATTACKERMULTICLASS($f, X, X_{\text{test}}; n$)

Sample $X^c \stackrel{\$}{\leftarrow} X, X_{\text{test}}^c \stackrel{\$}{\leftarrow} X_{\text{test}}$ s.t. $|X^c| = |X_{\text{test}}^c| = n$

$$X_{in}^a = \begin{bmatrix} f_0(x_0) | f_1(x_0) | \dots | f_k(x_0) | \text{onehot}(y_0) \\ f_0(x_1) | f_1(x_1) | \dots | f_k(x_1) | \text{onehot}(y_1) \\ \vdots \\ f_0(x_n) | f_1(x_n) | \dots | f_k(x_n) | \text{onehot}(y_n) \end{bmatrix}, \begin{bmatrix} 1 \\ 1 \\ \vdots \\ 1 \end{bmatrix}$$

$$X_{out}^a = \begin{bmatrix} f_0(x'_0) | f_1(x'_0) | \dots | f_k(x'_0) | \text{onehot}(y'_0) \\ f_0(x'_1) | f_1(x'_1) | \dots | f_k(x'_1) | \text{onehot}(y'_1) \\ \vdots \\ f_0(x'_n) | f_1(x'_n) | \dots | f_k(x'_n) | \text{onehot}(y'_n) \end{bmatrix}, \begin{bmatrix} 0 \\ 0 \\ \vdots \\ 0 \end{bmatrix}$$

for all $x_i, y_i \in X^c$ and $x'_i, y'_i \in X_{\text{test}}^c$.

$a \leftarrow \text{train} \left(\begin{bmatrix} X_{in}^a \\ X_{out}^a \end{bmatrix} \right)$

return a

Table S1: Model hyper-parameters. NB, LR, NN use scikit-learn notation. LR-AMP-DP uses the notation of Iyengar et al. [14]. LR-PSGD-DP uses notation of Wu et al. [27]. XGBoost uses the notation defined by its Python library interface.

| Model | Hyper-parameters |
|--------------------|--|
| LR | $C = 0.01$ |
| SVM | $C = 0.01, \text{kernel} = \text{“rbf”}$ |
| NN-6 | $\alpha = 0.01, \text{solver} = \text{“adam”}$ |
| NN-50 | $\text{solver} = \text{“adam”}$ |
| NN-100 | $\text{solver} = \text{“adam”}$ |
| NN-500 | $\text{solver} = \text{“adam”}$ |
| LR-AMP-DP | $\varepsilon = 1, \delta = \frac{1}{ X ^2}, L = 1,$ $\varepsilon_2 = 0.01 \cdot \varepsilon, \delta_2 = 0.01 \cdot \delta,$ $\varepsilon_3 = 0.9 \cdot (\varepsilon - \varepsilon_2),$ $\Lambda = 0$ |
| LR-PSGD-DP | $\varepsilon = 1, \delta = \frac{1}{ X ^2}, L = 1,$ $\mu_{\text{const}} = 0.001, \lambda = 0,$ $b = 50, k = 100$ |
| XGBoost (attacker) | $\text{learning_rate}=0.1, \text{max_depth}=2,$ $\text{min_child_weight}=14, \text{n_estimators}=100,$ $\text{subsample}=0.35$ |

For Approximate Minima Perturbation, we use the “hyperparameter-free” strategy suggested by Iyengar et al. [14]; and for Private Perturbation-based Convex SGD we use the default parameters provided in the implementation by Iyengar et al..

To pick the attacker’s model parameters, we use the tpot framework⁴ for genetic-programming-based model search. We run the search using 10 generations and 20 samples per generation on a random in/out sample with outputs of the LR model as the target model. As a viable alternative, we also consider k -Nearest Neighbours, choosing parameters independently for each attack simulation using 5-fold cross-validation with $k \in \{10, 20, 30, 40, 50, 60, 70, 80\}$. Even though k -Nearest Neighbours classifier obtains similar accuracy on non-compromised samples, it overfits to its training data (e.g., 90% accuracy on a compromised sample vs. 51% accuracy on a non-compromised sample).

S5.2 Synthetic Datasets

Table S2 shows (1) the performance of the target models, (2) MIA-privacy loss values and the privacy loss disparities across subgroups, averaged over 30 experiment runs, and (3) attack accuracy values and attack accuracy disparities across subgroups, averaged over 30 attack simulations.

On the Disparity in MIA-Privacy Loss vs. Disparity in Attack Accuracy We observe high MIA-privacy-loss disparity yet *no* significant attack-accuracy disparity on the disparate dataset X_D . The reason for this is that MIA-privacy losses provide a stronger, more pessimistic vulnerability estimate than our attack simulations can achieve.

In this synthetic experiment, we generate the datasets X_D and X_{ND} controlling only for the subgroup-sampling bias. Recall that MIA-privacy loss can be decomposed into a quantity that represents the

⁴<https://github.com/EpistasisLab/tpot>

Table S2: Results on Disparate synthetic dataset X_D (top), and Non-Disparate synthetic dataset X_{ND} (bottom). Columns: *Test acc.*—accuracy of the target model on the test dataset, *Train acc.*—accuracy of the target model on the train dataset; *Loss*—MIA-privacy loss \bar{L}^{MIA} , average over 30 replications; *Loss disp.*—max. absolute difference (*disparity*) in MIA-privacy loss \bar{L}_z^{MIA} between any two subgroups z, z' ; *Attack acc.*—accuracy of a simulated attacker, average over 30 attacks; *Attack disp.*—max. absolute difference (*disparity*) in attack accuracy between any two subgroups.

| Model | Test acc. | Train acc. | Loss | Loss disp. | Attack acc. | Attack disp. |
|--------|-----------|------------|-------|------------|-------------|--------------|
| LR | 0.101 | 0.115 | 0.356 | 0.321 | 0.729 | 0.036 |
| NN-6 | 0.101 | 0.112 | 0.440 | 0.323 | 0.744 | 0.077 |
| NN-50 | 0.097 | 0.150 | 0.621 | 0.337 | 0.777 | 0.036 |
| NN-500 | 0.101 | 0.218 | 0.743 | 0.321 | 0.653 | 0.032 |
| LR | 0.100 | 0.111 | 0.274 | 0.168 | 0.699 | 0.063 |
| NN-6 | 0.102 | 0.112 | 0.466 | 0.170 | 0.916 | 0.035 |
| NN-50 | 0.103 | 0.151 | 0.494 | 0.261 | 0.710 | 0.100 |
| NN-500 | 0.101 | 0.221 | 0.692 | 0.230 | 0.653 | 0.021 |

amount of overfitting for a particular group G_z , and the quantity that represents the subgroup-sampling bias.

Recall that the standard attacker [21, 26] we consider in our simulation only looks at the target model outputs (p) and the corresponding true classes (y) to distinguish between in- and out-of-training samples. When restricted to only these observations, the adversary does not have any information about the subgroup-membership of a target example, hence the modified subgroup-membership bias for G_z in X_D does not change the attacker’s accuracy on G_z compared to that on X_{ND} . The reason for disparate vulnerability for our simulated attacker can only be due to the disparity in overfitting across subgroups, which we do not control in our synthetic dataset experiments.

A stronger attacker that takes as input not only the true class and target outputs, but also the subgroup membership (z) for a given example, could observe disparity in our controlled scenario with X_D . Our goal in this work, however, is to investigate the disparate vulnerability that arises *even* when the attacker is not subgroup-aware.

S5.3 Details for Evaluation on Realistic Data

In this section, we provide the plots that show the results on ADULT-10 for all the models we considered. Figure S1 shows MIA-privacy losses and Figure S2 shows the attack accuracy values. To provide a more detailed picture of attacks’ disparity, we additionally present the results for attacker’s true-positive rates in Figure S3, and false-positive rates in Figure S4.

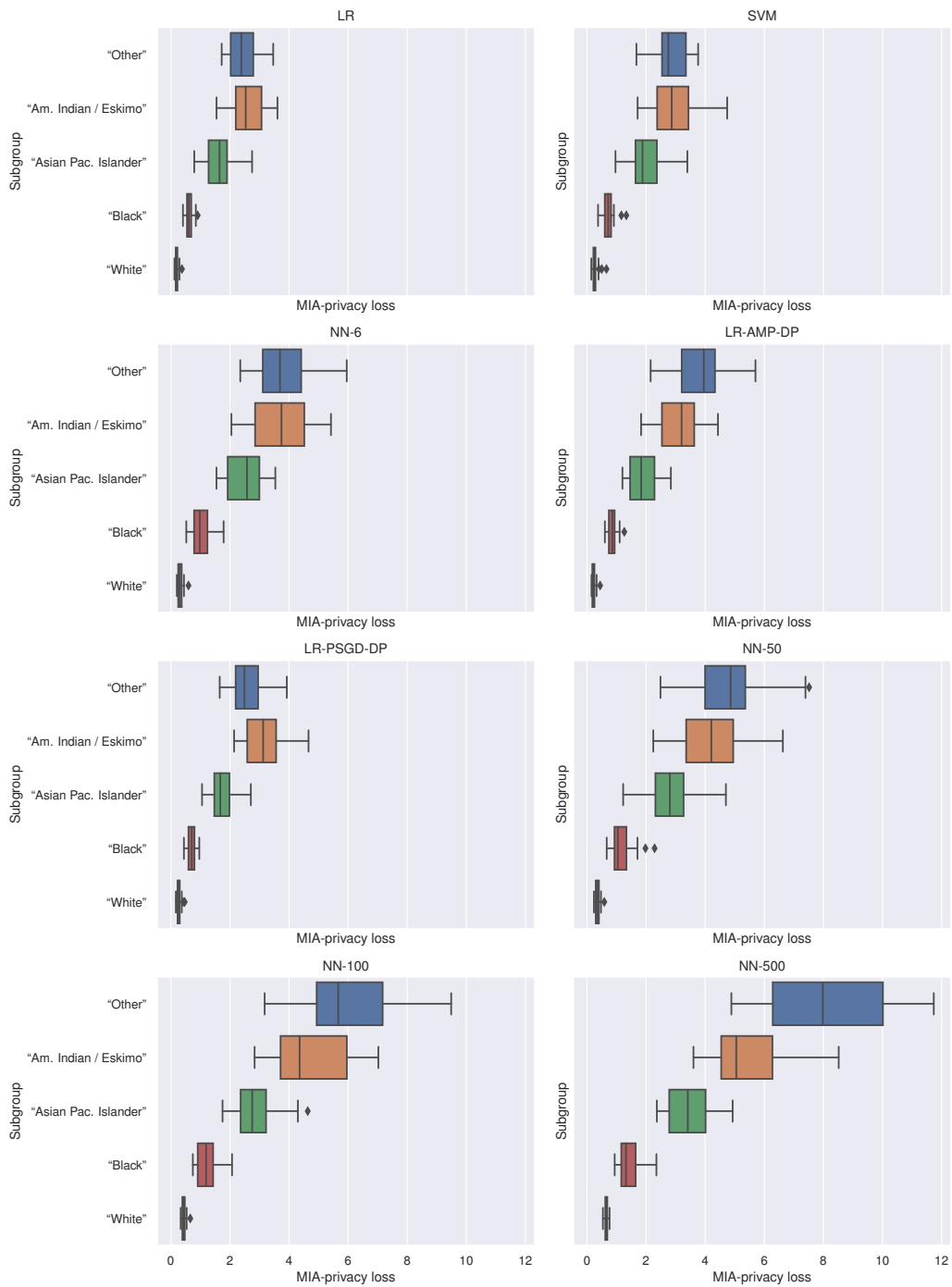


Figure S1: MIA-privacy losses on the ADULT-10 dataset. Lower loss means more privacy.

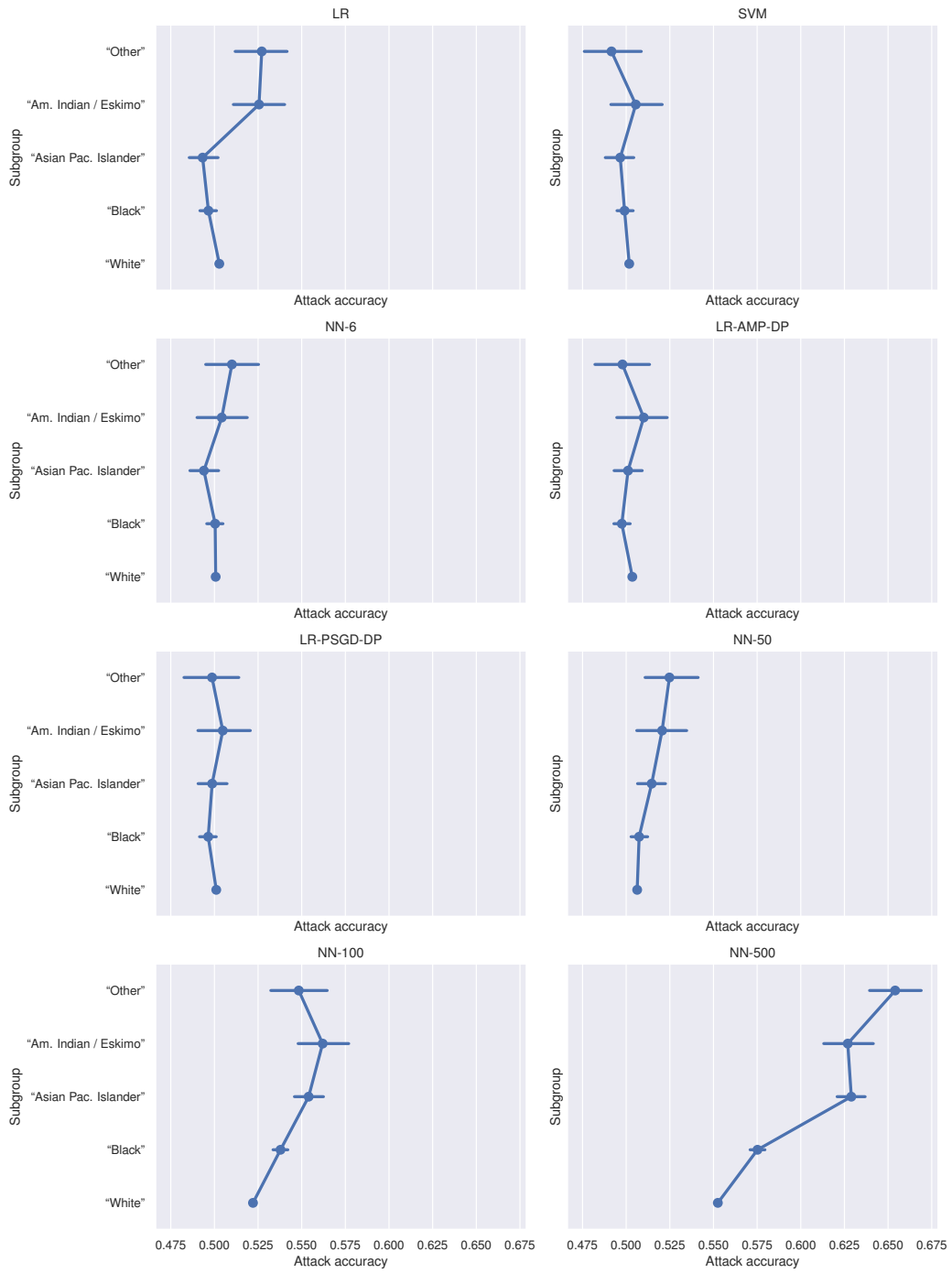


Figure S2: Simulated-attack accuracy on the ADULT-10 dataset. Higher accuracy means less privacy. Error bars represent 95% bootstrap CI over the full set of measurements.

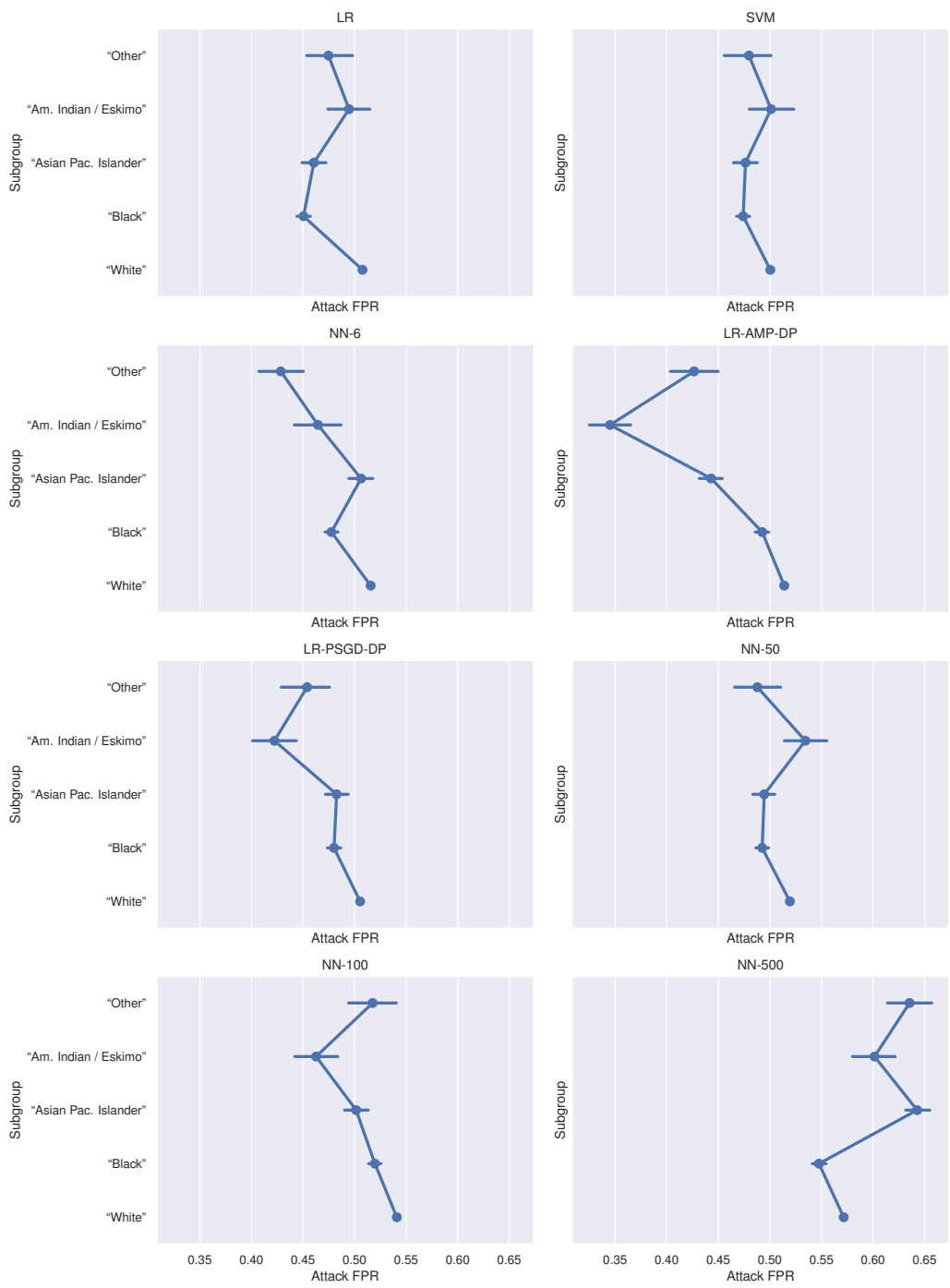


Figure S3: Simulated-attack true-positive rate (TPR) on the ADULT-10 dataset. Higher TPR means less privacy. Error bars represent 95% bootstrap CI over the full set of measurements.

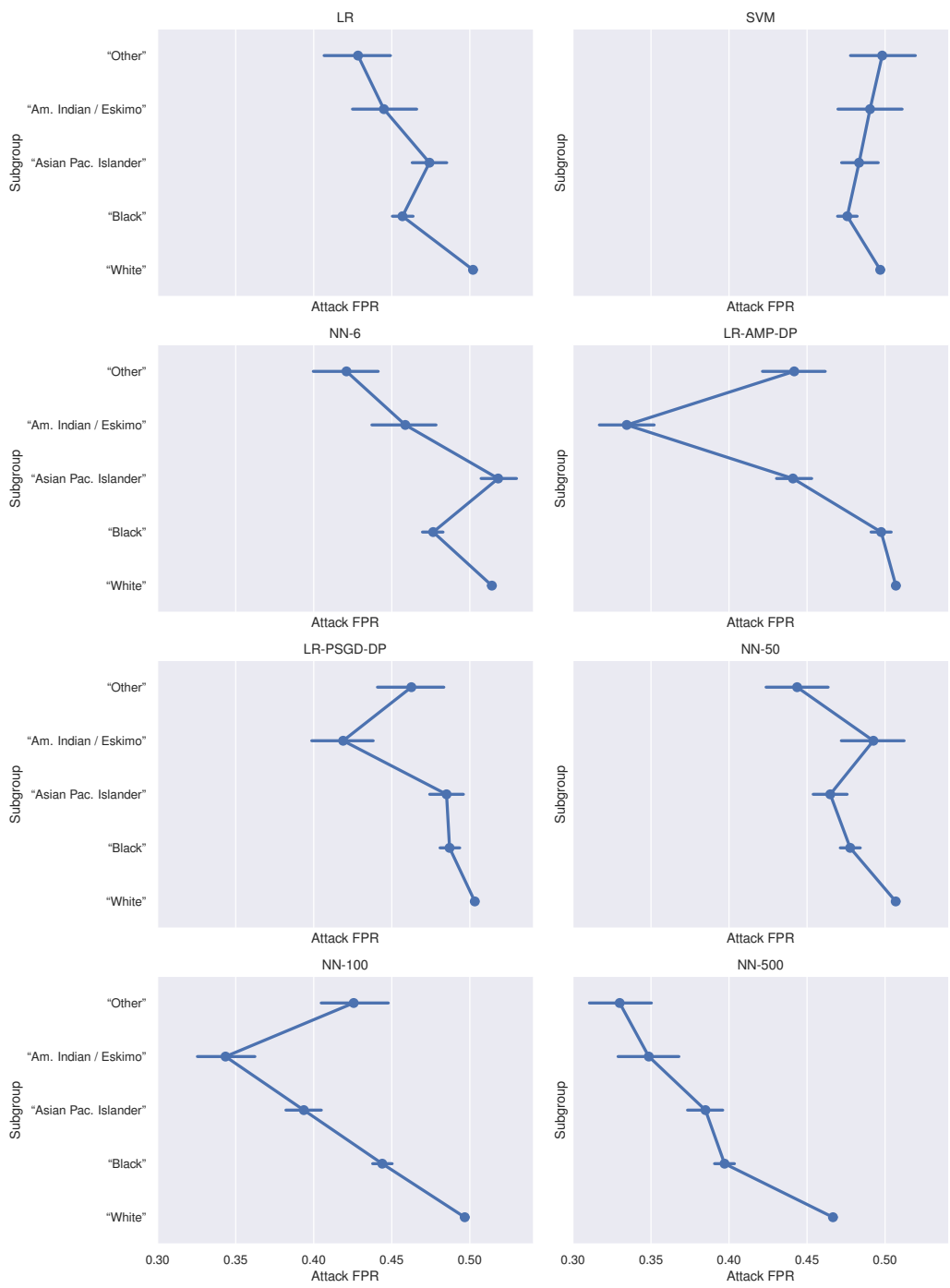


Figure S4: Simulated-attack false-positive rate (FPR) on the ADULT-10 dataset. Higher FPR means more privacy. Error bars represent 95% bootstrap CI over the full set of measurements.